Amino Acids (2011) 40:77–90
DOI 10.1007/s00726-010-0481-y

ORIGINAL ARTICLE

Investigating the effect of different positioning of lysine residues along the peptide chain of mastoparans for their secondary structures and biological activities

Bibiana Monson de Souza · Marcia Perez dos Santos Cabrera · João Ruggiero Neto · Mario Sergio Palma

Received: 9 December 2009 / Accepted: 8 January 2010 / Published online: 28 January 2010

Abstract In order to investigate the effect of the different positions of the positive charges generated by the ionization of the side-chain of lysine residues, on the structure–activity relationship of the mastoparans, the peptides Protonectarina-MP (INWKALLDAAKKVL-NH2), Parapolybia-MP (INWKKMAATALKMI-NH2) and Asn-2-Polybia-MP I (INWKKLLDAAKQIL-NH2) and MK-578 (INWLKAKKVAGMIL-NH2) were investigated as models. Thus, the four peptides had their secondary structure studied and were submitted to assays of mast cell degranulation, hemolysis, and antibiosis. The results of the bioassays made clear that those peptides bearing the positive charges positioned at the positions 4/5 and/or from 11 to 13 are the most active ones; meanwhile, the localization of the positive charges in the middle of peptide chain resulted in a poorly active peptide. Thus, Protonectarina-MP, Parapolybia-MP, and Asn-2-Polybia-MP I presented physiologically important hemolysis and antibiosis, while MK-578 presented only a reduced antibiotic activity. Circular dichroism analysis were carried-out in different environments revealing that the anionic environment of a mixture of phosphatidylcholine and phosphatidylglycerol (70:30) liposomes favored the higher helical content of the four peptides in this study in relation to the zwiterionic environment of 100% phosphatidylcholine liposomes. The positioning of the lysine residues at the strategic positions (4/5 and 11–13), flanking and maintaining stable α-helix which extends from the 4th to the 13th residue along the peptide chain, seems to contribute to maximal lytic efficiency of the mastoparans, which in turn results in a more homogeneous hydrophobic surface in the amphipathic structure.

Keywords Mastoparans · Antibiotic peptides · Hemolysis · Lysine-rich peptides · Circular dichroism

B. M. de Souza · M. S. Palma (✉)
CEIS/Department of Biology, Institute of Biosciences of Rio Claro, São Paulo State University (UNESP), Avenue 24-A no 1515, Bela Vista, 13506-900 Rio Claro, SP, Brazil
e-mail: mspalma@rc.unesp.br

M. P. dos Santos Cabrera · J. R. Neto
Department of Physics, IBILCE, UNESP, São José do Rio Preto, SP, Brazil

Introduction

Hymenoptera venoms are complex mixtures of biochemically and pharmacologically active components such as biogenic amines, peptides, and proteins (Nakajima et al. 1986).

Polycationic peptides constitute the largest group of toxins in the venoms of social and solitary wasps, which generally are amidated at their C-terminal residues (Xu et al. 2006; Murata et al. 2009). Mastoparans (De Souza et al. 2004), antimicrobial peptides (Mendes et al. 2004a), chemotactic peptides (Mendes et al. 2004b), and wasp kinins (Nakajima 1986) have been identified in these venoms.

Some mastoparans mimics the G-protein coupled receptor and can bind to this protein (Jones and Howl 2006; Watt 2002) which are involved in the activation of different types of basophils, such as mast cells and platelets, causing the delivering of histamine and serotonin, respectively (Nakajima et al. 1986; Oliveira et al. 2005; Rocha et al. 2008). These peptides may adopt amphipathic α-helical conformations in membrane-mimetic conditions (Dos Santos Cabrera et al. 2004) or in a membrane-bound state (Todokoro et al. 2006). These structural features contribute

to their interaction with the anionic components of the bacterial membranes, facilitating their assembly and the subsequent formation of pores in these membranes (Gallo and Huttner 1998). Because of this, some mastoparans also have antimicrobial activity (Krishnakumari and Nagaraj 1997; Mendes et al. 2004a, b). Antimicrobial peptides (AMPs) are important components of the non-specific host defense and innate immunity systems of different animal groups, including insects (Mitsuhara 2001). Turilazzi et al. (2006) demonstrated the importance of the mastoparans to prevent the infection of the colonies of social wasps from bacterial infections. The AMPs have inspired the development of novel antimicrobial agents, against resistant microorganisms. Many investigations have been performed focusing the design of novel peptides presenting increased antimicrobial activity, compared to the natural peptides used as models, without damaging the cells of the host organisms, generally mammals (Javadpour et al. 1996). The improvement of the antimicrobial activity has been tried in order to eliminate the cytotoxicity against mammalian cells, such as erythrocytes, just by changing physico-chemical parameters of these peptides such as chain length, amphipathicity, content of α-helix and net positive charge (Dathe and Wiprecht 1999; Dathe et al. 2002). The specific mechanism of action of mastoparans on membranes is not fully understood, requiring more detailed investigation; these toxins are amidated tetradecapeptides presenting α-helical conformations, with either two, or three (or even four) lysine residues in their sequences (Nakajima 1986). Certainly, the number and distribution of these amino acid residues along the sequence influence the amphipathicity and net positive charge of the peptides, which in turn affect the interaction of the mastoparans with the membranes.

To investigate the effect of the positive charge location in the structure and biological properties of the mastoparans, we selected a group of peptides presenting three lysine residues at different sequence positions. The present work reports the structural and functional characterization of three natural mast cell degranulating peptides, previously described in the literature as occurring in the venoms of social wasps: Protonectarina-MP (Dohtsu et al. 1993), Parapolybia-MP (Nakajima 1986) and Ans-2-Polybia-MP I (De Souza et al. 2005). In addition to this, an engineered mastoparan (MK-578) was also included in this study. The peptides were synthesized on solid-phase using Fmoc chemistry, and their secondary structures were determined both in the soluble form and as proteoliposomes with PC and PC/PG liposomes. Mast cell degranulation, hemolysis and antibiosis were assayed for these peptides in their soluble form. The four mastoparan peptides formed amphipathic α-helix conformations under membrane-mimetic conditions, presented reduced mast cell degranulation, intense hemolysis, and pronounced antimicrobial activity against both Gram-positive and Gram-negative bacteria.

Materials and methods

Peptide synthesis

The peptides Protonectarina-MP (INLWKALLDAA KKVL-NH2), Parapolybia-MP (INWKKMAATALKMI-NH2), and Asn-2-Polybia-MP I (INWKKLLDAAKQIL-NH2) were chosen due to the positioning of their Lys residues, as being good representatives of the mastoparan class, while MK-578 (INWLKAKKVAGMIL-NH2) was engineered locating the residues of lysine in the center of the peptide chain.

The peptides were prepared by step-wise manual solid-phase synthesis using *N*-9-fluorophenylmethoxy-carbonyl (Fmoc) chemistry with Novasyn TGS resin (NOVABIOCHEM). Side-chain protective groups included *t*-butyl for serine and *t*-butoxycarbonyl for lysine. Cleavage of the peptide-resin complexes was performed by treatment with trifluoroacetic acid/1,2-ethanedithiol/anisole/phenol/water (82.5:2.5:5:5:5 by volume), using 10 mL per gram of complex at room temperature for 2 h. After filtering to remove the resin, anhydrous diethyl ether (SIGMA) at 4°C was added to the soluble material causing precipitation of the crude peptide, which was collected as a pellet by centrifugation at 1,000*g* for 15 min at room temperature. The crude peptides were dissolved in water and chromatographed under RP-HPLC using a semi-preparative column (SHISEIDO C18, 250 × 10 mm, 5 μm), under isocratic elution with different concentrations of the mobile phase for each peptide: 53% (v/v) acetonitrile in water [containing 0.1% (v/v) trifluoroacetic] for Protonectarina-MP, 58% (v/v) acetonitrile in water [containing 0.1% (v/v) trifluoroacetic] for Parapolybia-MP, 60% (v/v) acetonitrile in water [containing 0.1% (v/v) trifluoroacetic] for Asn-2-Polybia-MP I and 48% (v/v) acetonitrile in water [containing 0.1% (v/v) trifluoroacetic] for MK-578. The elution was monitored at 214 nm with a UV-DAD detector (SHIMADZU, mod. SPD-M10A), and each fraction eluted was manually collected into 1.5 mL glass vials. The homogeneity and correct sequence of the synthetic peptides were assessed using a gas-phase sequencer PPSQ-21A (SHIMADZU) based on automated Edman degradation chemistry and ESI-MS analysis.

ESI mass spectrometry

Mass spectrometric analysis were performed in a triple quadrupole mass spectrometer (MICROMASS, mod.

Quattro II). The experimental protocol was based on previously described methods (Mendes et al. 2005) and adapted to the present investigation. The mass spectrometer was outfitted with a standard probe electrospray (ESI, MICROMASS, ALTRINCHAN, UK). The samples were injected into the electrospray transport solvent with a micro syringe (250 μL) coupled to a micro infusion pump (KD SCIENTIFIC) at a flow rate of 4 μL/min.

The mass spectrometer was calibrated with intact horse heart myoglobin and its typical cone-voltage induced fragments to operate at resolution 4,000. The samples were dissolved in 50% (v/v) acetonitrile [containing 0.1% (v/v) formic acid] to be analyzed by positive electrospray ionization (ESI+) using typical conditions: a capillary voltage of 3.5 kV, a cone-voltage of 30 V, a desolvation gas temperature of 80°C and flow of nebulizer gas (nitrogen) about 20 L/h and drying gas (nitrogen) 200 L/h. About 50 pmol of each sample was injected into the electrospray transport solvent. The ESI mass spectra were obtained in the continuous acquisition mode, scanning from m/z 100 to 2,500 at a scan time of 7 s. The data were acquired and treated using MassLynx software (MICROMASS).

Amino acid sequencing

The amino acids were sequenced using a gas-phase sequencer PPSQ-21A (SHIMADZU, Kyoto, Japan) based on automated Edman Degradation Chemistry.

Liposome preparation

Homogeneous films of lipids or lipid mixtures, made free from solvent traces, were obtained from zwitterionic egg L-α-phosphatidylcholine (PC) and anionic egg L-α-phosphatidyl-DL-glycerol (PG), at the following molar ratios: 100% PC, and a mixture of PC and PG, at 70:30 (named PCPG). Phospholipids were dissolved in a small volume of chloroform (1–2 mL), evaporated under N_2 flux in round bottom flasks, forming phospholipid films which were completely dried under vacuum for at least 3 h. Next they were hydrated with 5 mM Tris/H_3BO_3 buffer, containing 0.5 mM EDTA and 150 mM NaCl, pH 7.5 thorough vortex mixing to obtain a final phospholipid concentration around 10 mM.

The suspension was sonified with a titaniun tip sonifier (40 W) under N_2 flux in an ice/water bath for 50-min (or until clear) to produce small unilamellar vesicles (SUVs). Titanium debris was removed by centrifugation. Liposomes were used immediately after preparation. The lipid concentration was determined by phosphorus analysis (Rouser et al. 1970).

Circular dichroism (CD) measurements

CD spectra were obtained at 20 μM peptide concentration in different environments: 40% (v/v) 2,2,2-trifluoroethanol (TFE)/bi-distilled water, sodium dodecyl sulfate solutions (SDS), above and below the critical micellar concentration (cmc) (8 mM and 165 μM, respectively),100 μM PC and 100 μM PCPG liposomes. CD spectra were recorded from 260 to 190 nm with a Jasco-710 spectropolarimeter (JASCO International Co. Ltd., Tokyo, Japan), which was routinely calibrated at 290.5 nm using d-10-camphorsulfonic acid solution. Spectra were acquired at 25°C using 0.5 cm path length cell and averaged over nine scans at a scan speed of 20 nm/min, bandwidth of 1.0 nm, 0.5 s response and 0.1 nm resolution. Following baseline correction, the observed ellipticity, θ (mdeg) was converted to mean residue ellipticity $[\Theta]$ (deg cm^2/dmol) using the relationship: $[\Theta] = 100\theta/(lcn)$; where l is the path length in centimeters, c is peptide millimolar concentration, and n the number of peptide bonds. Assuming a two-state model, the observed mean residue ellipticity at 222 nm (Θ_{222}^{obs}) was converted into α-helix fraction (f_α) using the method proposed by Rohl and Baldwin (1998).

Molecular modeling

The modeling procedure began with an alignment of the target peptide sequence with Mastoparan-X (PDB id.: 2CZP), a related peptide of known three-dimensional (3D) peptide structure, as a template (Todokoro et al. 2006). Homologous structures for the peptides Polybia-MP-II and Polybia-MP-III amongst known structural templates in the PDB (Protein Data Bank) were identified using BLASTP (Schäffer et al. 2001; Altschul et al. 1997). This alignment was formatted as input for the program MODELER. The output is a 3D model for each target sequence containing all main-chain and side-chain non-hydrogen atoms. Several slightly different models can be calculated by varying the initial structure. To build the models, it was used the MODELLER 8 v.2, a program that uses a restrained-based modeling approach for comparative protein structure modeling (Sali and Blundell 1993). For each peptide, a total of 1,000 models were created, and the stereochemical quality of the models was assessed by the program PROCHECK (Laskowsky et al. 1993). The final models were selected with 100% residues in favored regions of the Ramachandran plot, with the best values of the overall G-factor and the lower values of energy minimization. For the visual inspection and to construct images of the molecular models of both peptides, the graphics programs MolMol (Koradi et al.1996) and VMD 1.8.6 (Humphrey et al. 1996) were used.

Molecular dynamics (MD) simulations

The MD calculations and trajectory analysis were performed using the AMBER (assisted model building with energy refinement) suite of programs running on a DELL Pentium IV (3.2 GHz) multiprocessor. Molecular visualization procedures were carried out using the INSIGHT II graphical environment on an Octane 2 workstation.

Simulation parameters

The calculations were performed by using the GROMACS all-hydrogen force field. The simulations were made using periodic boundary conditions with a cut-off radius of 0.8 nm for short-range interactions and updating the neighbor pair list for every 10 steps. Long range electrostatic interactions were treated with the Particle Mesh Ewald method (Darden et al. 1993; Cheatham et al. 1995). The algorithm LINCS (Hess et al. 1997) was used to constrain all bond lengths, while SETTLE (Miyamoto and Kollman 1992) was used to constrain water geometries. A time step of 5 fs was chosen for integrating the equations of motion. The simulations were performed at a constant temperature (293 K) and pressure (1 bar).

Simulation protocol

A canonical α-helix conformation was used as a starting model for the peptides Protonectarina-MP-NH2, Parapolybia-MP-NH2, Asn-2-Polybia-MP-NH2 and MK-578. The solvated peptides were submitted to an initial relaxation of solvent and ions through 500 steps of the steepest descents algorithm, while keeping the peptide backbone coordinates fixed. After the constraints had been removed, the systems were submitted to another short minimization step and the molecular dynamics simulations proceeded without any restraint for 10 ns. The atomic positions were recorded every 10 ps throughout each trajectory.

Biological activities

Mast cell degranulation

Degranulation was determined by measuring the release of the granule marker, β-D-glucosaminidase, which co-localizes with histamine, as previously described by Mendes et al. (2005). Mast cells were obtained by peritoneal washing of female adult Wistars rats. The mast cells were washed three times by re-suspension and centrifugation in a mast cell medium [150 mM NaCl (MERCK), 4 mM KCl (MERCK), 4 mM NaH_2PO_4 (SYNTH), 3 mM KH_2PO_4 (SYNTH), 5 mM glucose (SYNTH), 15 µM BSA (SIGMA), 2 mM $CaCl_2$ (MERCK), and 50 µL Liquemine (5,000 UI/0.250 mL) (ROCHE)]. The cells were incubated with various peptide concentrations for 15 min at 37°C, and after centrifugation, the supernatants were assayed for β-D-glucosaminidase activity. Briefly, 50 µL of substrate (5 mM *p*-nitrophenyl-*N*-acetyl-β-D-glucosaminidine in 0.2 M citrate, pH 4.5) and 50 µL of samples of the medium were incubated in 96-well plates for 6 h at 37°C to yield the chromophore *p*-nitrophenol. After incubation, 50 µL of the previous solution was added to 150 µL of 0.2 M Tris, and absorbance was measured at 405 nm. The values were expressed as the percentage of total β-D-glucosaminidase activity from rat mast cell suspensions, determined in lysed mast cells in the presence of 0.1% (v/v) Triton X-100 (considered as 100% reference). The results were compared to the activities measured for the standard mast cell degranulating peptide HR2 (SIGMA). The incubation of cells suspensions without any additives was the negative control. Results are expressed as mean ± SD of five experiments.

Hemolysis

Five hundred microliters of washed rat red blood cells (WRRBC) were suspended in 50 mL of physiological saline solution [0.9% (w/v) NaCl]. Ninety microliters of this suspension was incubated with 10 µL of peptide solution at different concentrations, at 37°C for 2 h. The samples were then centrifuged, and the absorbance of the supernatants were measured at 540 nm. The absorbance measured from lysed WRRBC in the presence of 1% (v/v) Triton X-100 was considered to be 100%. Results are expressed as mean ± SD of five experiments.

Antimicrobial activity

The minimal inhibitory concentrations (MIC) of the peptides were determined based on methods described by Meletiadis et al. 2000. The following microorganisms were used:

Bacilus subtilis (CCT 2576), *Staphylococcus aureus* (ATCC 6538), *Escherichia coli* (ATCC 25922), and *Pseudomonas aeruginosa* (ATCC 15422). The experiment was performed in 96-well plates. Bacterial cells were suspended in sterile culture medium; the inoculums size was 1×10^4 cells/mL in Müller–Hinton broth (DIFCO), confirmed by the use of McFarland scale. From this culture, 50 µl was spread onto the micro plate previously containing 50 µL of Müller–Hinton broth, resulting in a final cell density of 1.5×10^3 cell/mL. Cells were incubated at 37°C for 18 h in the presence of 100 µL of each peptide solution, in a concentration range of 0.8–50 µg/mL. After incubation, 10 µl of a triphenyltetrazolium chloride (TTC) (MALLINCKRODT) solution

(final concentration 0.05% w/v) was added to each well plate. The plates were incubated at 37°C for 24 h and after 20 μL of a triphenyltetrazolium chloride solution (TTC) 0.5% (w/v) was added. The plates were then incubated for an additional period of 2 h at 37°C. The minimal inhibitory concentration was that where the dye was not reduced; tetracycline in a concentration range from 0.2 to 600 μg/mL was used as control. Results are expressed as mean ± SD of five experiments.

Results

Peptide synthesis and purification

Protonectarina-MP and Parapolybia-MP were originally reported in the venom of the wasps *Protonectarina sylveirae* (Dohtsu et al. 1993) and *Parapolybia indica* (Nakajima 1986), while Asn-2-Polybia-MP I is a modification of Polybia-MP I found in the venom of *Polybia paulista* (De Souza et al. 2005). The peptide MK-578 was designed to have the lysine residues located at the positions 5, 7, and 8.

Peptides were manually synthesized on solid-phase and purified under reversed phase chromatography (results not shown). The homogeneity of each synthetic peptide was checked by ESI-MS analysis, and their sequences were obtained by using protocols of Edman degradation chemistry and MS/MS analysis.

ESI-MS spectrum of the peptide Protonectarina-MP (Fig. 1a) revealed three peaks of m/z 1,581.40, 790.87, and 527.59, corresponding to the molecular ions of the peptide as $[M + H]^+$, $[M + 2H]^{+2}$, and $[M + 3H]^{+3}$, respectively. The ESI-MS spectrum of Parapolybia-MP (Fig. 1b) showed the peaks of m/z 1,617.27, 809.13, and 539.74, corresponding to the molecular ions of the peptide as $[M + H]^+$, $[M + 2H]^{+2}$, and $[M + 3H]^{+3}$, respectively. The ESI-MS spectrum of Asn-2-Polybia-MP (Fig. 1c) showed the peaks of m/z 1,653.27, 826.93, and 551.71, corresponding to the molecular ions of the peptide as $[M + H]^+$, $[M + 2H]^{+2}$, and $[M + 3H]^{+3}$, respectively. The ESI-MS spectrum of MK-578 (Fig. 1d) showed the peaks of m/z 1,583.99, 791.58, and 528.73, corresponding to the molecular ions of the peptide as $[M + H]^+$, $[M + 2H]^{+2}$, and $[M + 3H]^{+3}$, respectively. A careful observation of the ESI-MS spectra reveals the presence of a single peptide component in each fraction, pure enough to be used in structural and functional studies. The deconvolution of the ESI-MS spectra shown in Fig. 1a–d reveals that the molecular masses of 1,580.40, 1,616.27, 1,652.27, and 1,582.99 Da, for the peptides Protonectarina-MP, Parapolybia-MP, Asn-2-Polybia-MP I, and MK-578, respectively. Therefore, the experimental masses of these peptides fit exactly the theoretical masses considering their C-termini in the amide form.

Secondary structure determination

Table 1 shows peptide sequences emphasizing the position of Lys residues: 4, 11, and 12; 4, 5, and 12; and 4, 5, and 11; which are typical of mastoparan peptides (Nakajima et al. 1986; De Souza et al. 2005). Other common features are the N-terminus INW sequence and the amidated C-terminus proceeded by a hydrophobic residue. The secondary structures of Protonectarina-MP, Parapolybia-MP, Asn-2-Polybia-MP I, and MK-578 were investigated by CD spectroscopy. Spectra of these peptides in water (Fig. 2) and Tris/H_3BO_3 buffer pH 7.5 (Fig. 3) are characteristic of unordered conformations. In 40% (v/v) TFE and in 8 mM SDS, the presence of two negative dichroic bands around 208 and 222 nm (Fig. 2) were observed, which is consistent with the induction of α-helix conformations in these peptides. SDS solutions below the cmc tends to induce β-sheet conformations and mimics the interior of proteins (Blondelle et al. 1997); sequences with lower helical propensities or presenting any tendency to

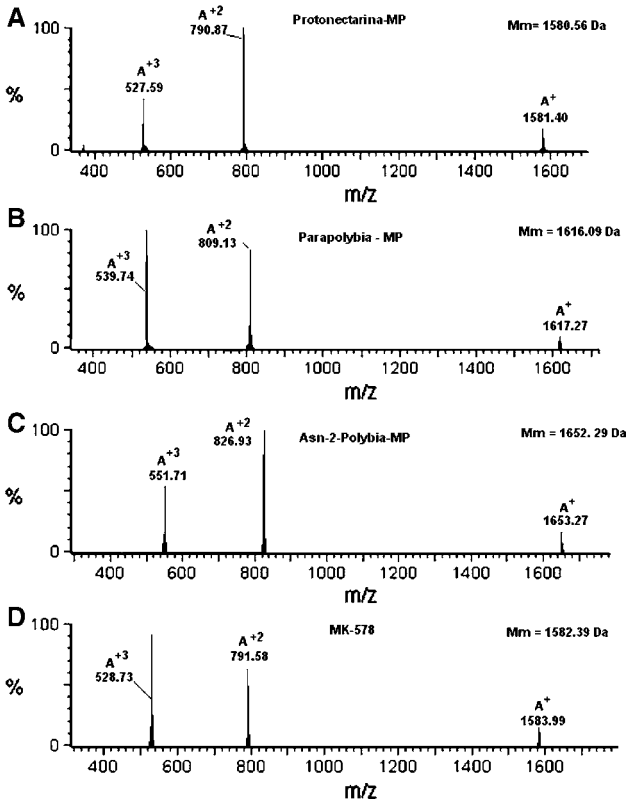

Fig. 1 ESI mass spectra in the positive mode, obtained for the synthetic peptides after their purification: Protonectarina-MP (**a**), Parapolybia-MP (**b**), Asn-2-Polybia-MP I (**c**), and MK-578 (**d**). For the recording of the spectrum 160 pmol of each peptide was used

Table 1 Sequences of the four mastoparan peptides investigated in the present study, compared to other mastoparans peptides from the literature, followed by the respective values of net charge (Q), mean hydrophobicity <H>

		Q	<H>
Protonectarina-MP	Ile-Asn-Trp-**Lys**-Ala-Leu-Leu-Asp-Ala-Ala-**Lys-Lys**-Val-Leu-$\mathbf{NH_2}$	+3	−0.05
Parapolybia-MP	Ile-Asn-Trp-**Lys-Lys**-Met-Ala-Ala-Thr-Ala-Leu-**Lys**-Met-Ile-$\mathbf{NH_2}$	+4	−0.03
Asn-2-Polybia-MP I	Ile-Asn-Trp-**Lys-Lys**-Leu-Leu-Asp-Ala-Ala-**Lys**-Gln-Ile-Leu-$\mathbf{NH_2}$	+3	−0.10
MK-578	Ile-Asn-Trp-Leu-**Lys**-Ala-**Lys-Lys**-Val-Ala-Gly-Met-Ile-Leu-$\mathbf{NH_2}$	+4	0.03
HR2	Phe-Leu-Pro-Leu-Ile-Leu-Gly-**Lys**-Leu-Val-**Lys**-Gly-Leu-Leu-$\mathbf{NH_2}$	+3	0.22
EMP-AF	Ile-Asn-Leu-Leu-**Lys**-Ile-Ala-Gly-**Lys**-Ile-Ile-**Lys**-Ser-Leu-$\mathbf{NH_2}$	+4	0.05
Polybia-MP1	Ile-Asp-Trp-**Lys-Lys**-Leu-Leu-Asp-Ala-Ala-**Lys**-Gln-Ile-Leu-$\mathbf{NH_2}$	+2	−0.11
MP-X	Ile-Asn-Trp-**Lys**-Gly-Ile-Ala-Ala-Met-Ala-**Lys-Lys**-Leu-Leu-$\mathbf{NH_2}$	+4	0.01

Based on the helical wheel projection

form aggregates will deviate from the helical pattern. The spectra obtained in this environment indicate almost the same level of ordered structures as those observed in SDS above the cmc, except for Parapolybia-MP that deviated from the characteristic negative dichroic bands at 208 and 222 nm. Figure 3 shows CD spectra of the peptides obtained at peptide/lipid molar ratio (P/L) of 0.2. In the presence of zwitterionic PC liposomes it was observed a drastic decrease in the peptides' ellipticity, especially Parapolybia-MP and MK578 that show spectra characteristic of unordered structures. In the presence of anionic PCPG liposomes there is also a reduction of ellipticity, but the spectra obtained are characteristic of α-helices. Table 2 presents the molar ellipticity ($[\Theta_{222}]$) and the percentage of α-helix calculated according to the two-state model (Rohl and Baldwin 1998) in the different environments: Protonectarina-MP, Parapolybia-MP, and Asn-2-Polybia-MP I showed the same helical content in the anionic 8 mM SDS solution probably due to the very similar positioning of their Lys residues in the chain; the helical content of these peptides in 40% TFE solution shows a slight difference, which may reflect the presence of an Asp residue at the eighth position in Protonectarina-MP and Asn-2-Polybia-MP I. The fact that Polybia-MP I, with similar Lys residues distribution, presents also 42.3% α-helix in SDS 8 mM and 41% in 40% TFE solution suggests that these environments should induce equivalent conformations in these peptides. Meanwhile MK-578, with Lys residues positioned in the middle of the chain presents considerably lower helical content in these mimetic media, which does not vary when brought in contact with PCPG liposomes and shows unordered structure in zwitterionic PC liposomes. The much lower helical content of these peptides in zwitterionic PC liposomes suggests poor binding, due to unfavorable electrostatic interactions with the bilayer, repulsive interactions between peptide monomers and their low hydrophobicity. Considering the interaction of peptides with similar Lys residues distribution with anionic PCPG vesicles, their respective helical contents seem to reflect a balance between hydrophilic (electrostatic) and hydrophobic contributions. Amongst the peptides with the same net charge +3, Protonectarina (<H> = −0.05), shows higher helical content than Asn-2-Polybia-MP-1, which is more hydrophilic (<H> = −0.10). The same was observed for the peptides with net charge +4, to which the most hydrophobic MK-578 is more structured in anionic vesicle than the hydrophilic Parapolybia.

Molecular modeling

The secondary structures of Protonectarina-MP, Parapolybia-MP, Asn-2-Polybia-MP I, and MK-578 were also analyzed by molecular modeling; 1,000 models were generated and validated through the analysis of the structure by the Procheck program (Laskowsky et al. 1993); this analysis considered the Ramachandran plot and values of the overall G-factor. Ideally, the value of this factor should be above −0.5; the values of G-factor for all models were between 0.25 and 0.28. In all models, 100% of the residues are in the most favored regions of the Ramachandran plot, with 10 residues in the α-helical region and only a single residue at the non-favored region (results not shown). The residues at the amino-/carboxyl-termini and the glycine residue are not considered because they can be localized in any region of the diagram. Figure 4a–h show the molecular models of these peptides as charge surface distribution, where the Fig. 4a, c, e and g represent the most hydrophobic surfaces, while the Fig. 4b, d, f, and h represent the most hydrophilic ones, revealing the amphipathic nature of these peptides. A careful observation of these models reveals that the hydrophobic surfaces were not completely homogenous, due the presence of a few hydrophilic side chains positioned in these surfaces, for the different molecular models (Fig. 4a, c, e, g).

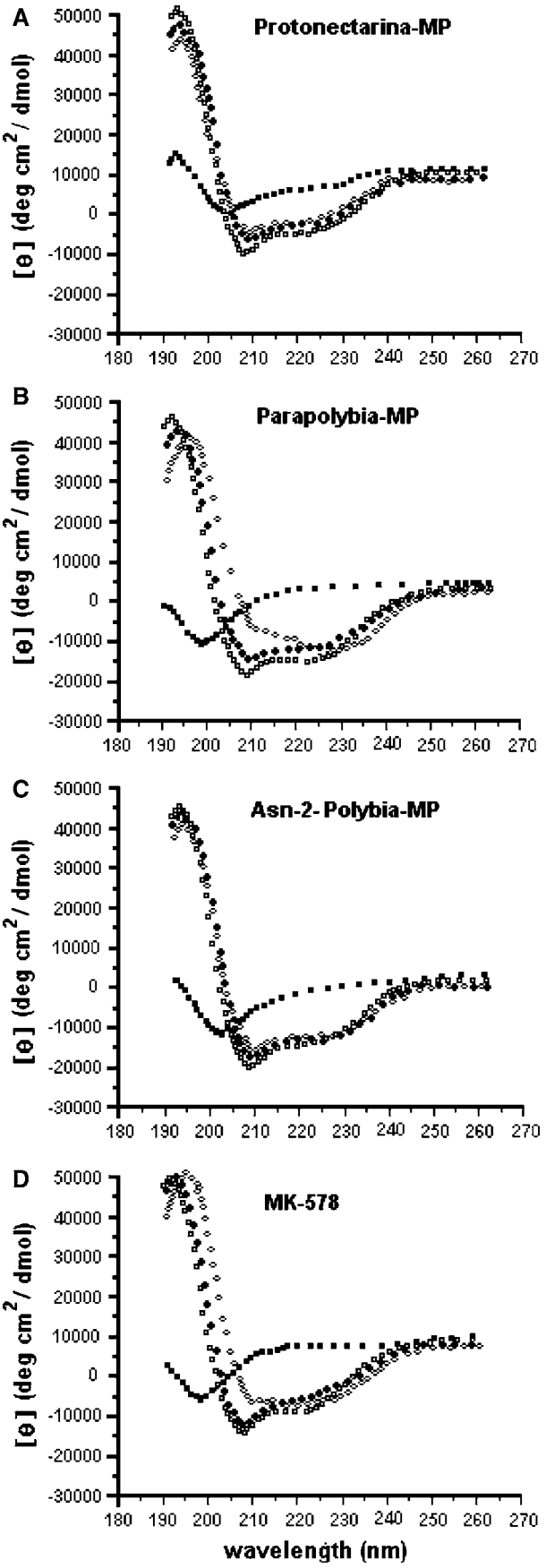

◀ **Fig. 2** CD spectra of the peptides (20 μM) Protonectarina-MP (**a**), Parapolybia-MP (**b**), Asn-2-Polybia-MP I (**c**) and MK-578 (**d**) at 25°C in the presence of: water (*closed square*), 40% TFE (*open square*), 165 μM SDS; (*oval shaped*) and 8 mM SDS (*plus symbol*)

MD Simulations

The flexibility of Protonectarina-MP, Parapolybia-MP, Asn-2-Polybia-MP, and MK-578 were studied in a solvent simulating environment of 30:70 TFE/H2O mixture (v/v), during 10 ns for each peptide.

The simulations started with Protonectarina-MP, Parapolybia-MP-I, Asn-2-Polybia-MP, and MK-578 folded in a full ideal α-helix, obtained by the molecular modeling as described above. The root-mean-square deviations (RMSD) of the α-carbons backbone of the four peptides (Fig. 5) were calculated over the 10 ns of MD simulation. A careful observation of the profile of RMSD values along the 10 ns clearly indicates that the four peptides undergone large conformational changes in this period of time. The profile of RMSD values for Protonectarina-MP (Fig. 5A) reveals some periods of conformational stability, where about 71% of its amino acid residues were involved in helix formation, which is split into two segments in some moments of the simulation. The simulation trajectory of Parapolybia-MP shows a long period of stability, in which the peptide conformation is characterized by a continuous helix (Fig. 5b); after this period, large conformational changes are observed. The observation of the RMSD trajectory for Asn-2-Polybia-MP I (Fig. 5c) reveals a long period of conformational stability, in which the peptide presents a helical conformation split into two segments. The analysis of the trajectory of RMSD values for the peptide MK-578 shows only short periods of conformational stability; the helical conformation predominates all over the simulation. In order to obtain a contribution for the better understanding of the effective amphipathicity of molecules of Protonectarina-MP, Parapolybia-MP, Asn-2-Polybia-MP I, and MK-578, ten different conformational states of each peptide molecule observed during MD simulations, were overlapped as may be observed in Fig. 6. The overlapped structures were set to show the transversal view of the molecules from the N- to C-terminal residue of each peptide, showing the α-carbon backbones in the center, with the side chains of the lysine residues emphasized for each one of the ten conformational states.

Functional characterization

Biological activities of Protonectarina-MP, Parapolybia-MP, Asn-2-Polybia-MP I, and MK-578 were investigated by assaying mast cell degranulation, hemolysis, and antimicrobial activity. Figure 7 shows the results of rat

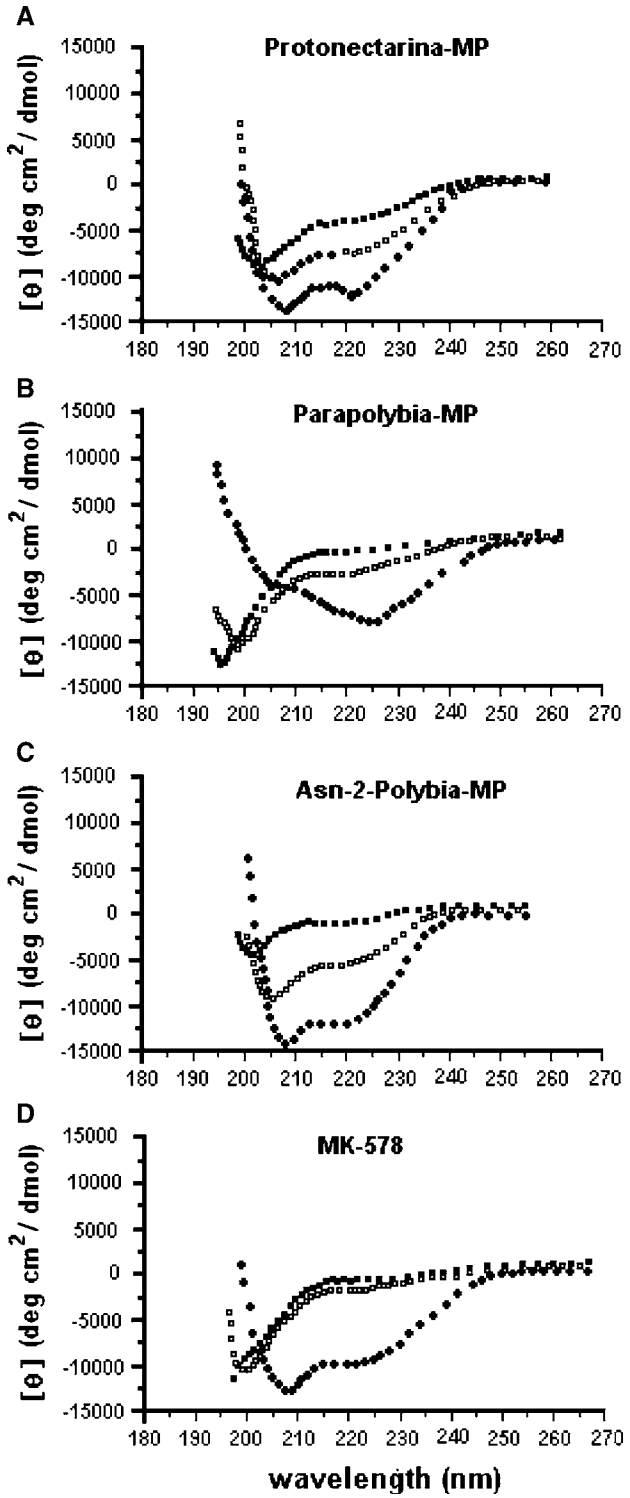

Fig. 3 CD spectra of the peptides (20 μM) Protonectarina-MP (**a**), Parapolybia-MP (**b**), Asn-2-Polybia-MP I (**c**) and MK-578 (**d**) at 25°C in the presence of: Tris–borate buffer pH 7.5 (*closed square*), PC liposomes (*open square*) and PC/PG (70/30) liposomes (*plus symbol*)

peritoneal mast cell degranulation as a function of the peptides' concentrations from 10^{-7} to 10^{-4} M. Results indicate that the peptides HR2 (standard reference), Asn-2-Polybia-MP I and Protonectarina-MP cause peritoneal mast cell degranulation with ED_{50} values of 7.0×10^{-4} M, 5.2×10^{-4} M and 4.0×10^{-4} M, respectively. The peptides Parapolybia-MP and MK-578 did not present enough activity to reach the ED_{50} values in the concentration range up to 10^{-4} M. In fact, the concentrations of peptides at which the ED_{50} values were observed are too high to consider that their actions are important under physiological conditions.

Figure 8 shows the hemolytic activity of the peptides as a function of their concentrations in the range of 10^{-7}–10^{-4} M. These results show that the peptides Protonectarina-MP, Parapolybia-MP, and Asn-2-Polybia-MP I cause hemolysis with values of ED_{50} equal to 3.4×10^{-5} M, 3.7×10^{-5} M, and 2.6×10^{-5} M, respectively; the standard peptide (HR2) presented $ED_{50} = 1.5 \times 10^{-6}$ M. These values of ED_{50} indicate that the peptides may produce significant hemolysis at physiological concentrations, while MK-578 is not a hemolytic peptide.

The results of the antimicrobial activities are summarized in Table 3. They indicate that Parapolybia-MP shows more potent antimicrobial activity against the Gram-positive and Gram-negative bacteria, than the other peptides. Protonectarina-MP, Parapolybia-MP, and Asn-2-Polybia-MP I are equally efficient against Gram-negative bacteria. Except for MK-578 the peptides of this study are more potent antibacterial agents than the standard antibiotic Tetracycline against the Gram-positive bacteria, and at least so potent as this compound in relation to the Gram-positive bacteria. The engineered peptide MK-578 is not an efficient antibacterial agent indicating that the positioning of the lysine residues (fifth, seventh and eighth) resulted in a strongly decreased antibacterial effect.

Thus, the three natural mastoparan peptides investigated are more potent than the other antimicrobial peptides from wasp venoms, reported in Table 3. In fact, they are more potent antimicrobial peptides than most polycationic peptides from Hymenoptera venoms reported by Krishnakumari and Nagaraj (1997), Konno et al. (2000) and Konno et al. (2001).

Discussion

The four peptides used in the present investigation were manually synthesized and extensively purified as demonstrated by the ESI-MS spectra (Fig. 1). Despite all the peptides present three lysine residues in their sequences, Parapolybia-MP and MK-578 present net positive charges +4, while Protonectarina-MP and Asn-2-Polybia-MP I presents net positive charges +3 (due to the presence of an aspartic acid residue in their sequences; see Table 1).

Table 2 Molar ellipticity at 222 nm ($[\theta]_{222}$) and α-helix fraction of the peptides in different environments

Environment	Protonectarina-MP		Parapolybia-MP		Asn-2-Polybia-MP I		MK-578	
	$[\Theta]_{222}$	% α-helix	$[\Theta]_{222}$	% α-helix	$[\Theta]_{222}$	% α-helix	$[\Theta]_{222}$	% α-helix
Water	−430.9	rc	−567.5	rc	−535.1	rc	−606.5	rc
165 μM SDS	−12,261.5	38.7	−12,616.5	39.8	−12,865.1	40.6	−8,885.3	27.6
8 mM SDS	−12,383.8	41.1	−12,997.5	41.1	−13,051.0	41.2	−7,554.6	23.2
TFE 40% (v/v)	−14,594.6	46.0	−15,209.1	48.4	−13,488.1	46.6	−9,417.0	29.3
TRIS buffer pH 7.5	−4,673.1	13.7	−1,926.6	rc	−1,294.3	rc	−1,568.7	rc
100 μM PC liposomes	−7,978.6	24.6	−3,781.5	10.8	−5,747.4	17.3	−2,098.1	rc
100 μM PCPG liposomes	−12,455.5	39.3	−7,484.9	23	−12,389.0	30.1	−8,977.6	27.9

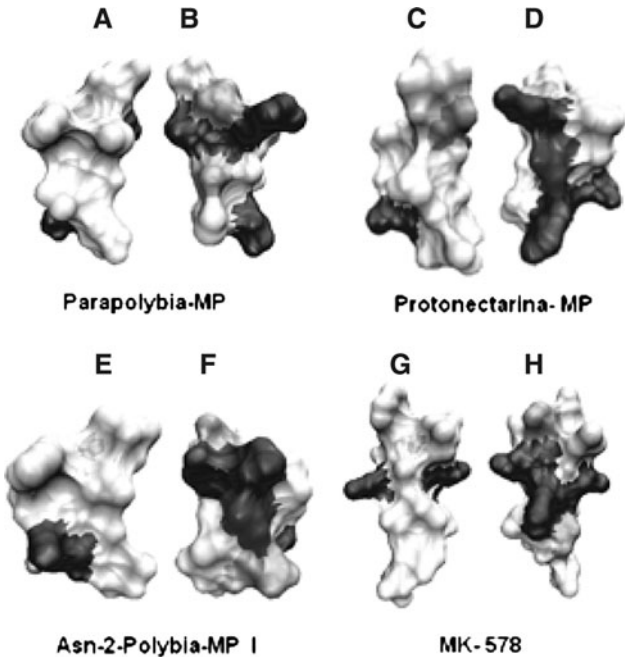

Fig. 4 Structural models of Parapolybia-MP (**a**, **b**), Protonectarina-MP (**c**, **d**), Asn-2-Polybia-MP I (**e**, **f**) and MK-578 (**g**, **h**) as charge surface representation: negative residues are shown in *black*, positive ones in *grey*, hydrophilic ones in *light grey* and hydrophobic ones in *white*

It has been demonstrated recently that the short, polycationic peptides of wasps venoms are multifunctional, presenting several biological activities (De Souza et al. 2009). Thus, the four peptides under investigation in the present study were assayed for mast cell degranulation, hemolysis, and antibiosis. The results of the bioassays shown in Figs. 7 and 8, and in Table 3 made clear that the peptides Protonectarina-MP, Parapolybia-MP, and Asn-2-Polybia-MP I are much more active than the engineered peptide MK-578. At first, this observation is indicating that those peptides bearing the positive charges distributed at the positions 4/5 and/or from 11 to 13 are the most active ones; meanwhile, the localization of the positive charges in the middle of peptide chain results in a poorly active peptide as observed for MK-578.

Circular dichroism analysis in different environments showed that these peptides undergo important conformational changes from random coil in aqueous solution to helical structures induced by anisotropic environments. The results reported above made clear that upon binding to the membrane surface, the short polycationic peptides often assume helical conformations and the degree of α-helix is directly related to the burial of the backbone into a more hydrophobic region and to their ability to disturb the membranes. The anionic micellar environment (SDS 8 mM) and the electrically neutral 40% (v/v) TFE solution induced approximately the same amount of secondary structures in the three natural peptides, suggesting that hydrophobic interactions may be more important than the electrostatic in inducing these conformational changes.

The anionic environment of PCPG lipossomes appeared to favor the higher helical content of Protonectarina-MP, Parapolybia-MP and Asn-2-Polybia-MP I (Table 2), than the zwiterionic environment of PC liposomes. This fact seems to correlates well with the antimicrobial activity of these peptides, which is indicative of their stronger interaction with the anionic bacterial membranes, than with the zwiterionic animal membranes. This observation became clear by comparing the greatness of the ED_{50} values obtained for mast cell degranulation (in the range of 10^{-4} M) and hemolysis (in range of 10^{-5} M), with the values of MIC obtained for the antibiosis (in the range of 10^{-6} M).

In addition to this, none of the four peptides investigated presented physiologically important mast cell degranulation activity (Fig. 5). Mast cell degranulation may occur either by the activation of G-protein mediated exocytosis, or through mast cell membrane lysis (Mendes et al. 2004a, 2005). The results above are indicating that neither the direct interaction of the four peptides with the zwiterionic membranes of the mast cells, nor their molecular recognition by the G-protein coupled receptors resulted in

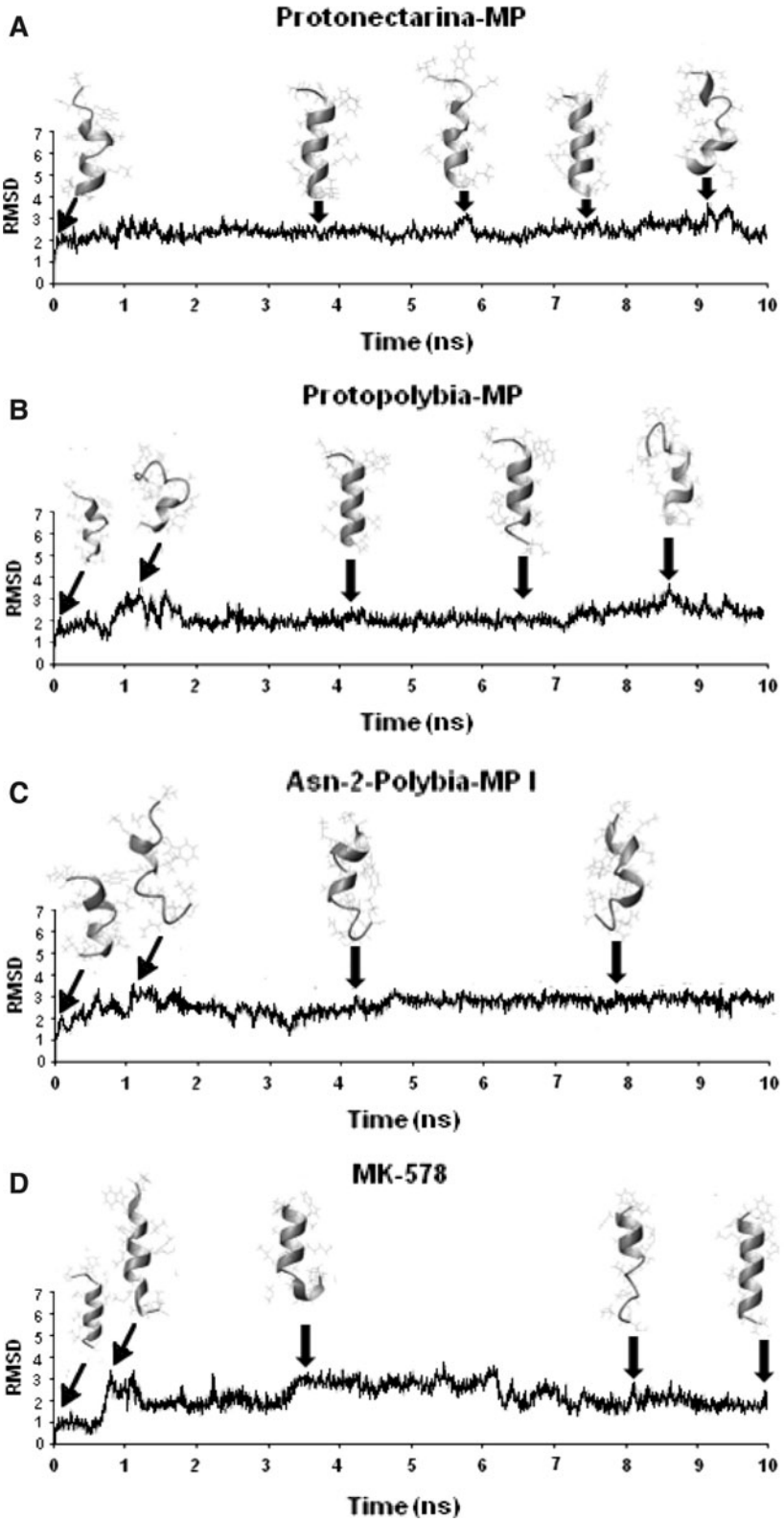

Fig. 5 Root-mean-square fluctuation (RMSD) of the backbone atoms Protonectarina-MP (**a**), Parapolybia-MP (**b**), Asn-2-Polybia-MP I (**c**) and MK-578 (**d**) along the 10 ns of each MD simulation in a 30:70 (v/v) TFE/H_2O mixture. In some specific times the secondary structure assumed by the peptides at that moments are shown

significant mast cell degranulation, suggesting that these peptides may present a higher affinity by the zwiterionic membranes of the erythrocytes, than by the membranes of mast cells.

NMR studies indicate that the helical portions of some mastoparan peptides lie between the 4th and 13th residues, which is a structural feature common to the most peptides of this family (Todokoro et al. 2006). Because of this, we

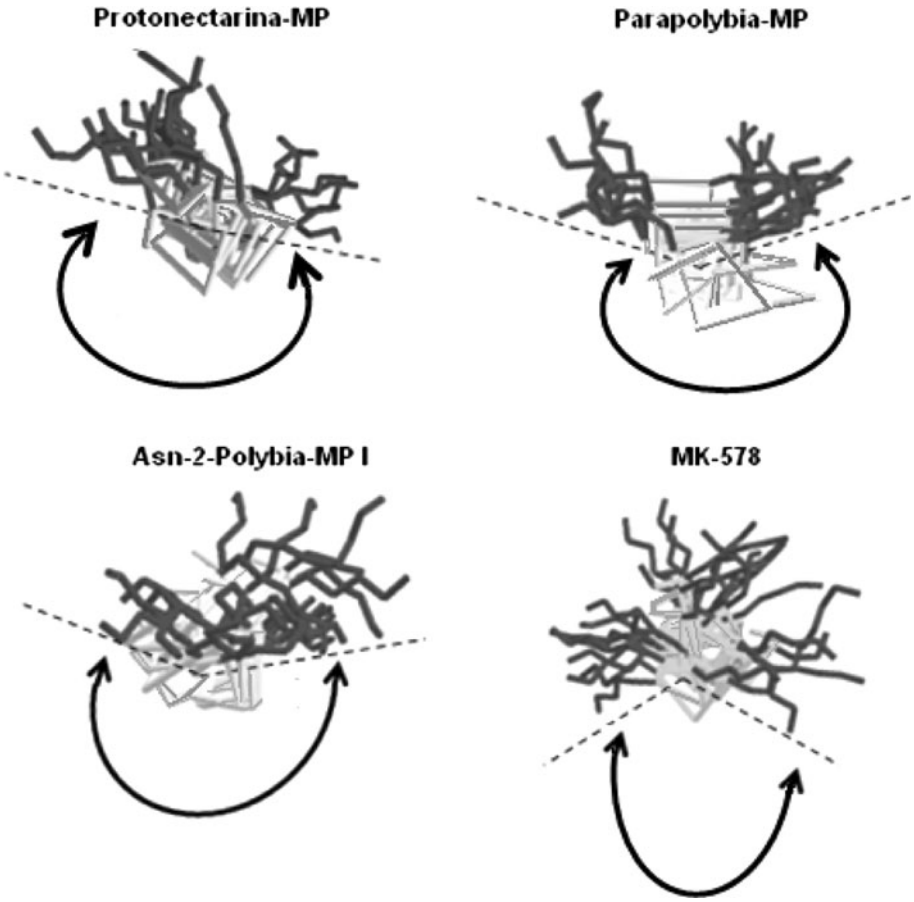

Fig. 6 Superposition of the final 10 calculated structures of Protonectarina-MP, Parapolybia-MP, Asn-2-Polybia-MP I, and MK-578 in a 30:70 (v/v) TFE/H_2O mixture based on the minimum pairwise RMSD of the peptide backbone (in *grey*), with the side chains of lysine residues (in *black*) at different positions assumed in each conformational state considered for this purpose. The assigned regions in the superimposed structures emphasizes the hydrophobic surface available for interaction with the core of membranes in each peptide

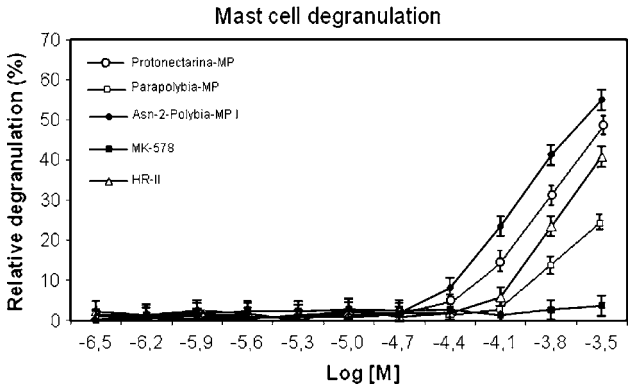

Fig. 7 Degranulation activity in rat peritoneal mast cells for the peptides Protonectarina-MP, Parapolybia-MP, Asn-2-Polybia-MP I and MK-578. The activity was determined by measuring the release of the granule marker, β-D-glucosaminidase, which co-localizes with histamine. The values for β-D-glucosaminidase released in the medium were expressed in the percentage of total enzyme activity. Values are mean ± SD ($n = 5$)

selected three natural mastoparans bearing the positive charges of the lysine residues flanking the helical portion of the molecules, i.e., at the positions 4/5 and/or from 11 to 13; in addition to this, a novel peptide (MK-578) was engineered in order to have the positive charges in the middle of the peptide chain. The G-factors and the Ramachandran plots (results not shown) for the molecular models generated for the four peptides are indicating that all the four structural models are stereochemically possible.

The tendency to form an amphipathic structure with a well defined hydrophobic surface, clearly distinct from the hydrophilic one, is characteristic of the mastoparans (De Souza and Palma 2008). This aspect is clearly observed in the molecular models shown in Fig. 4a, c and e, respectively, for Parapolybia-MP, Asn-2-Polybia-MP I, and Protonectarina-MP. Probably the more homogeneous hydrophobic surfaces of these peptides, favor their interaction with the acyl-chains of the phospholipids both of zwitterionic membranes of the animal cells and the anionic membranes of the bacterial cells. The positive charges of the lysine residues and of the N-terminus and/or the negative charges of aspartic acid residues may interact with the charges located at the surface of cell membranes. The location of the positive charges from the side chains of the lysine residues, at the positions 5, 7, and 8 seems to have disrupted the ideal amphipathic structure in the peptide MK-578 (Fig. 4g, h), creating an heterogeneous hydrophobic surface, which certainly decreases its interaction with the biological membranes.

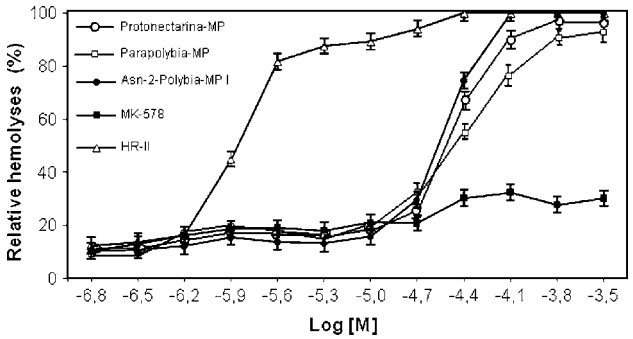

Fig. 8 Hemolytic activity in WRRBC for the peptides Protonectarina-MP, Parapolybia-MP, Asn-2-Polybia-MP I and MK-578. The absorbance measured at 540 nm from lysed WRRBC in presence of 1% (v/v) Triton X-100 was considered as 100%. Values are mean ± SD ($n = 5$)

Table 3 Antimicrobial activity of the peptides Protonectarina-MP, Parapolybia-MP, Asn-2-Polybia-MP I and MK-578

	Minimal inhibitory concentration (MIC) (μg/mL)			
	Gram-negative		Gram-positive	
PEPTÍDES	*E. coli*	*P. aeruginosa*	*S. aureus*	*B. subtilis*
Protonectarina-MP	7.8	62.5	3.9	3.9
Parapolybia-MP	3.9	15.6	2.9	3.5
Asn-2-Polybia-MP I	5.8	46.8	7.8	4.9
MK-578	23.4	125.0	42.9	11.7
Tetracycline	15.6	93.7	2.4	15.6
EMP-AF[a]	50.0	20.0	5.0	–
Eumenitin[b]	9.8	48.8*	>98.0	>98.0**

[a] Konno et al. (2000)

[b] Konno et al. (2006)

[c] ATCC15442

[d] CCT2471

Figure 6 shows clearly that the peptides Protonectarina-MP, Parapolybia-MP, and Ans-2-Polybia-MP I present one side of their molecules (about half of the molecule diameter) completely filled by the movements of the side chain of lysine residues, while the other side is not filled by the side chain of any hydrophylic amino acid residue. These results support the hypothesis that the molecules of these peptides present about half of their molecular surface filled by hydrophilic groups, while the other half is hydrophobic one, attributing an amphipathic nature of these peptides. This aspect favors the interaction of these molecules with the biological membranes, explaining the relatively high hemolytic and antimicrobial activities of these peptides. Meanwhile, the peptide MK-578 presents about 70% of its molecular surface filled by the side chains of lysine residues, creating a large hydrophilic surface, against a reduced hydrophobic surface. Despite the molecule of MK-578 to have a tendency to be helical, its effectively reduced hydrophobic surface does not favor the interaction of this peptide with the biological membranes, which may explain the poor hemolytic and antimicrobial activities of MK-578.

Membrane lysis caused by the antimicrobial peptides is proposed to proceed by pore formation through one of the three known mechanisms: "carpet" (Shai 1999), "barrel stave" (Sansom 1991) and "wormhole" (Ludtke et al. 1996). The specific type of mechanism played by the mastoparans is not well known up to now, however, the positioning of the lysine residues at the strategic positions (4/5 and 11–13), flanking and maintaining stable the α-helix which extends from the 4th to 13th residue along the peptide chain, must contribute to maximal lytic efficiency of the mastoparans, which in turn results in a more homogeneous hydrophobic surface in the amphipathic structure. Perhaps, this is the reason why no natural mastoparan was reported up to now in the literature, presenting lysine residues located from the sixth to eighth positions of the peptide chain.

A series of biophysical aspects have been suggested to contribute for the interaction between the short polycationic peptides with biological membranes and/or membrane-mimetic systems, such as requirement of a minimal amount of positive charges, peptide chain helicity/hydrophobicity and hydrophobic moment (Eisenberg et al. 1984; Dathe et al. 1996; Dathe et al. 1997; Taheri-Araghi and Ha 2007; Dos Santos Cabrera et al. 2008; De Souza and Palma 2008; Dos Santos Cabrera et al. 2009). Thus, the knowledge about the location of lysine residues along the peptide sequence represents an important structural feature, which may improve the engineering of peptides in the search for novel and more selective antimicrobial agents.

Acknowledgments This research is supported by grants from FAPESP (BIOprospecTA Proc. 04/07942-2, 06/57122-6), CNPq and Instituto Nacional de Ciência e Tecnologia de Investigação em Imunologia- *iii* (INCT/CNPq-MCT). MSP and JRN are researchers for the Brazilian Council for Scientific and Technological Development (CNPq).

References

Altschul SF, Madden TL, Schaffer AA, Zhang J, Zhang Z, Miller W, Lipman DJ (1997) Gapped BLAST and PSI-BLAST: a new generation of protein database search programs. Nucleic Acids Res 25:3389–3402

Blondelle SE, Forood B, Houghten RA, Perez-Paya E (1997) Secondary structure induction in aqueous vs membrane-like environments. Biopolymers 42:489–498

Cheatham TE, Miller JL, Fox T, Darden TA, Kollman PA (1995) Molecular dynamics simulations on solvated biomolecular systems: the Particle Mesh Ewald method leads to stable trajectories of DNA, RNA and proteins. J Am Chem Soc 117:4193–4194

Darden T, York D, Pedersen L (1993) Particle Mesh Ewald: an N-log(N) method for Ewald sums in large systems. J Chem Phys 98:10089–10092

Dathe M, Wiprecht T (1999) Structural features of helical antimicrobial peptides: their potential to modulate activity on model membranes and biological cells. Biochim Biophys Acta 1462:71–78

Dathe M, Schumann M, Wieprecht T, Winkler A, Beyermann M, Krause E, Matsuzaki K, Murase O, Bienert M (1996) Peptide helicity and membrane surface charge modulate the balance of electrostatic and hydrophobic interactions with lipid bilayers and biological membranes. Biochemistry 35:12612–12622

Dathe M, Wieprecht T, Nikolenko H, Handel L, Maloy WL, MacDonald DL, Beyermann M, Bienert M (1997) Hydrophobicity, hydrophobic moment and angle subtended by charged residues modulate antibacterial and haemolytic activity of amphipathic helical peptides. FEBS Lett 403:208–212

Dathe M, Meyer J, Beyermann M, Maul B, Hoischen C, Biernet M (2002) General aspects of peptide selectivity towards lipid bilayers and cell membranes studied by variation of the structural parameters of amphipathic helical model peptides. Biochim Byophys Acta 1558:171–186

De Souza BM, Palma MS (2008) Monitoring the positioning of short polycationic peptides in model lipid bilayers by combining hydrogen/deuterium exchange and electrospray ionization mass spectrometry. Biochim Biophys Acta 1778:2797–2805

De Souza BM, Marques MR, Tomazela DM, Eberlin MN, Mendes MA, Palma MS (2004) Mass spectrometric characterization of two novel inflammatory peptides from the venom of the social wasp *Polybia paulista*. Rap Commun Mass Spectrom 18:1095–1102

De Souza BM, Mendes MA, Santos LD, Marques MR, César LMM, Almeida RNA, Pagnocca FC, Konno K, Palma MS (2005) Structural and functional characterization of two novel peptide toxins isolated from the venom of the social wasp *Polybia paulista*. Peptides 26:2157–2164

De Souza BM, Silva AVR, Resende VMF, Arcuri HA, Dos Santos Cabrera MP, Ruggiero Neto J, Palma MS (2009) Characterization of two novel polyfunctional mastoparan peptides from the venom of the social wasp *Polybia paulista*. Peptides 30:1387–1395

Dohtsu K, Hagiwara K, Palma MS, Nakajima T (1993) Isolation and sequence analysis of peptides from the venom of *Protonectarina sylveirae* (Hymenoptera, Vespidae) (I). Nat Toxins 1:271–276

Dos Santos Cabrera MP, De Souza BM, Fontana R, Konno K, Palma MS, de Azevedo WF Jr, Ruggiero-Neto J (2004) Conformation and lytic activity of Eumenine Mastoparan: a new antimicrobial peptide from wasp venom. J Peptide Res 64:95–103

Dos Santos Cabrera M, Costa STB, de Souza BM, Palma MS, Ruggiero JR, Ruggiero Neto J (2008) Selectivity in the mechanism of action of antimicrobial mastoparan peptide Polybia-MP1. Eur Biophys J 37:879–891

Dos Santos Cabrera MP, De Souza BM, Ruggiero Neto J, Palma MS (2009) Interactions of mast cell degranulating peptides with model membranes: a comparative biophysical study. Arch Biochem Biophys 486:1–11

Eisenberg D, Schwarz E, Komaromy M, Wall R (1984) Analysis of membrane and surface protein sequences with the hydrophobic moment plot. J Mol Biol 179:125–142

Gallo RL, Huttner KM (1998) Antimicrobial peptides: an emerging concept in cutaneous biology. J Investig Dermatol 111:739–743

Hess B, Bekker H, Berendsen HJC, Fraaije JGEM (1997) LINCS: a linear constraint solver for molecularsimulations. J Comput Chem 18:1463–1472

Humphrey WF, Dalke A, Schulten K (1996) VMD, visual molecular dynamics. J Mol Graphics 14:33–38

Javadpour MM, Juban MM, Lo WC, Bishop SM, Alberty JB, Cowell SM, Becker CL, McLaughlin ML (1996) De novo antimicrobial peptides with low mammalian cell toxicity. J Med Chem 39:3107–3113

Jones S, Howl J (2006) Biological applications of the receptor mimetic peptide mastoparan. Curr Protein Pept Sci 7:501–508

Konno K, Hisada M, Naoki H, Itagaki Y, Kawai N, Miwa A, Yasuhara T, Morimoto Y, Nakata Y (2000) Structure and biological activities of Eumenine Mastoparan-AF (EMPAF), a new mast cell degranulating peptide in the venom of the solitary wasp (*Anterhynchium flavomarginatum micado*). Toxicon 38:1505–1515

Konno K, Hisada M, Fontana R, Lorenzi CCB, Naoki H, Itagaki Y, Miwa A, Kawai N (2001) Anoplin, a novel antimicrobial peptide from the venom of the solitary wasp *Anoplius samariensis*. Biochim Biophys Acta 1550:70–80

Konno K, Hisada M, Naoki H, Itagaki Y, Fontana R, Rangel M, Oliveira JS, Cabrera MP, Neto JR, Hide I, Nakata Y, Yasuhara T, Nakajima T (2006) Eumenitin, a novel antimicrobial peptide from the venom of the solitary eumenine wasp *Eumenes rubronotatus*. Peptides 27:2624–2631

Koradi R, Billeter M, Wüthrich K (1996) MOLMOL: a program for display and analysis of macromolecular structures. J Mol Graphics 14:51–65

Krishnakumari V, Nagaraj P (1997) Antimicrobial and hemolytic activities of Crabolin, a 13-residues peptide from the venom of the European hornet, *Vespa crabro*, and its analogs. J Peptide Res 50:88–93

Laskowsky RA, MacArthur MW, Moss D, Thornton JM (1993) PROCHECK: a program to check the stereochemical quality of protein structures. J Appl Crystallogr 26:283–291

Ludtke SJ, He K, Heller WT, Harroun TA, Yang L, Huang HW (1996) Membrane pores induced by magainin. Biochemistry 35:13723–13728

Meletiadis J, Meis JGM, Mouton JW, Donnelly VPE (2000) Comparison of NCCLS and 3-(4, 5-dimethyl-2-thiazyl)-2, 5-diphenyl-2Htetrazolium bromide (MTT) methods of in vitro susceptibility testing of filamentous fungi and development of a new simplified method. J Clin Microbiol 38:2949–2954

Mendes MA, De Souza BM, Marques MR, Palma MS (2004a) Structural and Biological characterization of two novel peptides from the venom of the neotropical social wasp *Agelaia pallipes pallipes*. Toxicon 44:67–74

Mendes MA, Souza BM, Santos LD, Palma MS (2004b) Structural characterization of novel chemotactic and mastoparan peptides from the venom of the social wasp *Agelaia pallipes pallipes* by high-performance liquid chromatography/electrospray ionization tandem mass spectrometry. Rapid Commun Mass Spectrom 18:636–642

Mendes MA, Souza BM, Palma MS (2005) Structural and biological characterization of three novel mastoparan peptides from the venom of the neotropical social wasp *Protopolybia exigua* (Saussure). Toxicon 45:101–106

Mitsuhara I (2001) In vitro growth inhibition of human intestinal bacteria by sarcotoxin IA, an insect bactericidal peptide. Biotechnol Lett 23:569–573

Miyamoto S, Kollman PA (1992) SETTLE: an analytical version of the SHAKE and RATTLE algorithm for rigid water models. J Comput Chem 13:952–962

Murata K, Shinada T, Ohfune Y, Hisada M, Yasuda A, Naoki H, Nakajima T (2009) Novel mastoparan and protonectin analogs isolated from a solitary wasp, *Orancistrocerus drewseni drewseni*. Amino Acids 37:389–394

Nakajima T (1986) Pharmacological biochemistry of vespid venoms. In: Piek T (ed) Venom of hymenoptera, 1st edn. Academic Press, London, pp 309–327

Nakajima T, Uzu S, Wakamatsu K, Saito K, Miyazawa T, Yasuhara T, Tsukamoto Y, Fujino M (1986) Amphiphilic peptides in wasp venom. Biopolymers 25:115–121

Oliveira L, Cunha AOS, Mortari MR, Coimbra NC, dos Santos WF (2005) Cataleptic activity of the denaturad venom of the social

wasp *Agelaia vicina* (Hymenoptera, Vespidae) in *Rattus norvegicus* (Rodentia, Muridae). Prog Neuro Psychopharmacol Biol Psych 30:198–203

Rocha T, Leonardo MB, De Souza BM, Palma MS, Da Cruz-Höfling MA (2008) Mastoparan effects in skeletal muscle damage: an ultrastructural view until now concealed. Microsc Res Tech 71:220–229

Rohl CA, Baldwin RL (1998) Deciphering rules of helix stability in peptides. Methods Enzymol 295:1–26

Rouser G, Fleischer S, Yamamoto A (1970) Two dimensional thin layer chromatographic separation of polar lipids and determination of phospholipids by phosphorus analysis of spots. Lipids 5:494–496

Sali A, Blundell TL (1993) Comparative protein modeling by satisfaction of spatial restraints. J Mol Biol 234:779–815

Sansom MP (1991) The biophysics of peptide models of ion channels. Prog Biophys Mol Biol 55:139–215

Schäffer AA, Aravind L, Madden TL, Shavirin S, Spouge JL, Wolf YI, Koonin EV, Altschul SF (2001) Improving the accuracy of PSI-BLAST protein database searches with composition-based statistics and other refinements. Nucl Acids Res 29:2994–3005

Shai Y (1999) Mechanism of the binding, insertion and destabilization of phospholipid bilayer membranes by alpha-helical antimicrobial and cell non-selective membrane-lytic peptides. Biochim Biophys Acta 1462:55–70

Taheri-Araghi S, Ha BY (2007) Physical basis for membrane-charge selectivity of cationic antimicrobial peptides. Phys Rev Lett 98:168101-1–168101-4

Todokoro Y, Yumen I, Fukushima K, Kang SW, Park JS, Kohno T, Wakamatsu K, Akutsu H, Fujiwara T (2006) Structure of tightly membrane-bound Mastoparan-X, a G-protein-activating peptide determined by solid-state NMR. Biophys J 91:1368–1379

Turilazzi S, Mastrobuoni G, Dani FG, Moneti G, Pieraccini G, La Marca G, Bartolucci G, Perito B, Perito B, Lambardi D, Cavallini VC, Dapporto L (2006) Dominulin A and B: Two new antibacterial peptides identified on the cuticle and in the venom of the social paper wasp *Polistes dominulus* using MALDI-TOF, MALDI-TOF/TOF and ESI-ion trap. J Am Mass Spectrom 17:376–383

Watt AP (2002) Mast cells and peptide induced histamine release. Inflammopharmacol 9:421–434

Xu X, Li J, Lu Q, Yang H, Zhang Y, Lai R (2006) Two families of antimicrobial peptides from wasp (*Vespa magnifica*) venom. Toxicon 47:249–253